Measurement of the 2*S* Hyperfine Interval in Atomic Hydrogen

N. Kolachevsky,* A. Matveev,* J. Alnis, C. G. Parthey, S. G. Karshenboim,† and T. W. Hänsch
Max-Planck-Institut für Quantenoptik, 85748 Garching, Germany

(Received 3 February 2009; published 28 May 2009)

An optical measurement of the 2*S* hyperfine interval in atomic hydrogen using two-photon spectroscopy of the 1*S*-2*S* transition gives a value of 177 556 834.3(6.7) Hz. The uncertainty is 2.4 times smaller than achieved by our group in 2003 and more than 4 times smaller than for any independent radio-frequency measurement. The specific combination of the 2*S* and 1*S* hyperfine intervals predicted by QED theory $8f_{\mathrm{HFS}}(2S) - f_{\mathrm{HFS}}(1S) = 48\,953(3)$ Hz is in good agreement with the value of 48 923(54) Hz obtained from this experiment.

DOI: 10.1103/PhysRevLett.102.213002 PACS numbers: 32.10.Fn, 12.20.Fv, 32.30.Jc, 42.62.Fi

Precision spectroscopy in simple atomic systems and predictions by quantum-electrodynamics theory (QED) supply essential data for the determination of fundamental constants [1–3]. The measurements also enable sensitive tests of the theory ensuring high confidence in the calculations. One type of test is based on hyperfine splitting (HFS) measurements in hydrogenlike systems.

In conventional atoms, the sensitivity of the HFS-based tests is restricted by an insufficient knowledge of their nuclear structure [4]. The corresponding uncertainty can be reduced by construction of the specific difference of the 2*S* and 1*S* HFS frequencies $D_{21} = 8f_{\mathrm{HFS}}(2S) - f_{\mathrm{HFS}}(1S)$ for which the nuclear size effects significantly cancel out [5–7]. The interest in the D_{21} calculations was inspired by the experiment of Heberle, Reich, and Kusch [8], and significant progress has been made recently [9]. The present theoretical uncertainty is due to fourth-order QED corrections such as $\alpha(Z\alpha)^2 m/M$ and $\alpha^2(Z\alpha^2)$ in units of $f_{\mathrm{HFS}}(1S)$ (α is the fine structure constant, Z is the nuclear charge number, and m/M is the electron-to-nucleus mass ratio). That is similar to HFS in muonium, the positronium spectrum, and the Lamb shift in H [5].

The 1*S* and 2*S* HFS frequencies are accurately measured in H, D, and $^3\mathrm{He}^+$. The lowest D_{21} relative uncertainty of 10 ppb [normalized by $f_{\mathrm{HFS}}(1S)$] is reached in the He^+ ion [10,11], while for H and D the uncertainty is about 100 ppb. The present sensitivity of these QED tests is mostly restricted by the experimental uncertainty of $f_{\mathrm{HFS}}(2S)$, since $f_{\mathrm{HFS}}(1S)$ is measured with much higher accuracy.

In 2003, we implemented an optical method for measuring the 2*S* HFS frequency in H by two-photon spectroscopy of the 1*S*-2*S* transition [12]. The result of 177 556 860(16) Hz improved the previous values [8,13] measured by radio-frequency spectroscopy. The calculation of D_{21} from the two most recent measurements [12,13] and the precisely measured value of $f_{\mathrm{HFS}}(1S) = 1\,420\,405\,751.768(1)$ Hz [14] showed a deviation from the theoretical prediction [$D_{21}^{\mathrm{theor}} = 48.953(3)$ kHz [9]] at the 2σ level (σ is the D_{21} uncertainty).

In this work we have remeasured $f_{\mathrm{HFS}}(2S)$ in H. The optical method relies on the measurement of the frequency difference between the two two-photon transitions $1S(F=0) \rightarrow 2S(F=0)$ (the *singlet* f_s) and $1S(F=1) \rightarrow 2S(F=1)$ (the *triplet* f_t) recorded sequentially in time [12]. The splitting is obtained from $f_{\mathrm{HFS}}(2S) = f_{\mathrm{HFS}}(1S) + f_t - f_s$ in a zero magnetic field.

As the most critical improvement compared to Ref. [12], we use a new ultrastable optical frequency reference [15]. Also, a reanalysis of the 2*S* HFS frequency pressure shift shows that it is negligible in our apparatus.

To measure $f_{\mathrm{HFS}}(2S)$, we sequentially excite the singlet and the triplet transitions by the second harmonic of a 486 nm dye laser [16] locked to the ultralow expansion (ULE) glass reference cavity 1 with a horizontal optical axis (Fig. 1). The dye laser has a linewidth of 60 Hz (for 0.2 s) and a frequency drift of about 1 Hz/s, while its frequency stability is 5×10^{-14} for 10^3 s (linear drift corrected).

To tune the dye laser frequency between the two hyperfine transitions, a double-pass acousto-optic modulator (AOM) is installed between cavity 1 and the laser. The required frequency detuning of 310 MHz is too big to tune the laser rapidly without taking it out of lock.

We take advantage of the excellent frequency stability of an external cavity diode laser (ECDL) at 972 nm locked to the thermally and vibrationally compensated ULE cavity 2 described in detail in Ref. [15]. It is stabilized at the zero expansion temperature such that the influence of external temperature fluctuations is strongly suppressed. The frequency drift is nearly linear with a slope of about +50 mHz/s. The ECDL has a linewidth of 0.5 Hz and a frequency stability of 4×10^{-15} in 10^3 s. The ECDL is continuously locked to cavity 2. Its frequency is monitored by a fiber frequency comb referenced to an active H maser to ensure correct operation.

The beat note frequency between the dye laser and the second harmonic of the ECDL is mixed down with a local oscillator (186 MHz) to the 30 MHz range and is then counted with a counter as shown in Fig. 1. All oscillators

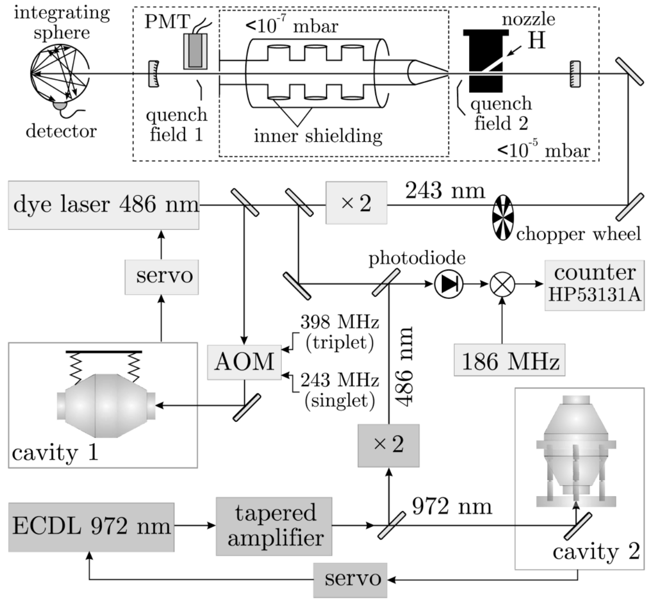

FIG. 1. Experimental setup. The dye laser locked to the ULE cavity 1 in horizontal configuration serves for spectroscopy of the $1S$-$2S$ transition in H. To switch between the singlet and the triplet transitions, the double-pass AOM frequency is changed. The 972 nm ECDL is continuously locked to the ULE cavity 2 in a vertical configuration and serves as an optical frequency reference. The beat note frequencies of 32 (triplet) and 29 MHz (singlet) are recorded by the counter simultaneously with the $1S$-$2S$ data.

are referenced to the Global Positioning System-disciplined H maser guaranteeing a fractional frequency uncertainty of 10^{-14}.

The measurement of the beat note frequency shows that the relocking of the dye laser causes two effects: First, after relocking, the dye laser frequency shows a strong nonlinear drift up to a few hertz per second due to transient thermal effects in cavity 1. Second, it causes abrupt random changes of the laser frequency of up to 100 Hz at 486 nm due to insufficient servo loop amplification at low frequencies. In 2003, we had no possibility to monitor the dye laser frequency during the measurement. The laser instability resulted in excessive data scatter and could cause a systematic shift. In the new measurement, the instability of the dye laser has basically no influence on the data quality, as the ECDL is never unlocked.

The second harmonic of the dye laser is coupled to a linear enhancement cavity forming a standing wave for Doppler-free two-photon spectroscopy. Atomic hydrogen produced in a microwave discharge is cooled down to 4–7 K by a copper nozzle and escapes along the cavity axis. Some of the atoms are excited to the $2S$ state during their flight. The $2S$ state is quenched in the detection region at a distance of 19.5 cm from the nozzle by an electric field of 10 V/cm (quench field 1). The $2S$ population is measured by counting the Lyman-α photons. Compensation coils together with μ-metal shielding suppress magnetic fields in the interrogation volume to less than 30 mG. A part of the volume (18 cm in length) is surrounded by additional magnetic shielding with a suppression factor of 300 which also serves as a beam collimator and Faraday cage. This shielding separates the high-vacuum region from the rest of the vacuum chamber. All parts of the apparatus surrounding the beam are coated with graphite to suppress stray electric fields.

Compared to Ref. [12], we use a cryogenic nozzle with a diameter of 2.2 mm which allows one to record H lines for up to 1 h without melting the frozen layer of H_2 on its inner surface. The film improves the $2S$ count rate, but at some thickness it blocks the 243 nm laser beam and should be melted. An electrode is installed close to the nozzle to optionally quench the $2S$ atoms excited within that region (quench field 2).

We use time-of-flight detection to study different velocity groups in the cold atomic beam. The 243 nm light is chopped at 160 Hz, and a multichannel scaler records counts falling into 12 time bins starting at $\tau = 10, 210, \ldots, 2210$ μs and finishing at 3 ms after the 243 nm light is closed by the chopper.

The UV power in the enhancement cavity is maintained nearly constant at the level of 300 mW per direction and is monitored by a calibrated photodiode installed after the output coupler. To prevent beam-pointing effects, we use an integrating sphere. The power fluctuations are taken into account by correction of the measured frequencies for the ac Stark shift which is evaluated by a Monte Carlo code

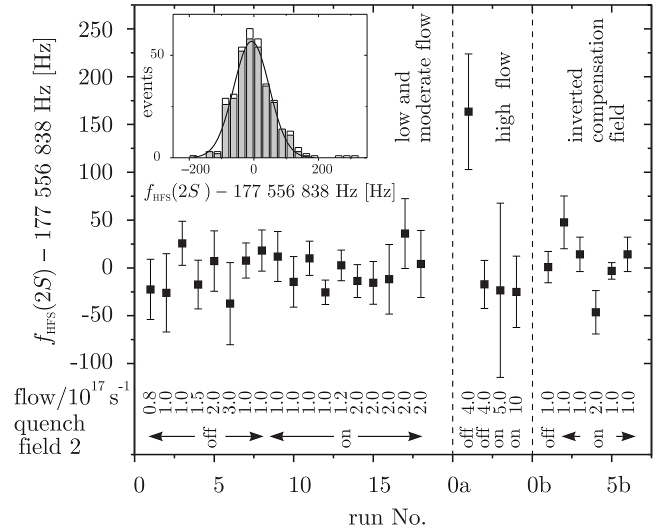

FIG. 2. $2S$ HFS frequency in H evaluated for $\tau = 810$ μs using the averaged line fit. Each data point is the average over one set of measurements at unchanged conditions (particle flow, quench field 2, compensation magnetic field). The histogram shows $f_{HFS}(2S)$ data for low and moderate particle flows (gray bars) and all data (white bars) except the ones taken with an inverted compensation field. The solid line is a Gaussian fit.

[17]. For $\tau = 810\ \mu$s, the ac Stark shift correction equals 1.3(1) Hz/mW.

The measurement sequence is the same as in Ref. [12]: Groups of 2–4 singlet or triplet spectra are recorded one after another, and the time t_0 and the AOM frequency corresponding to each line center are defined by a fit. We use either a Lorentzian fit or an unsymmetrical line shape obtained by averaging all superimposed and amplitude-normalized experimental line shapes for each τ (“averaged line fit”). The lines are fitted by the averaged line fit for the given τ using 3 parameters: the amplitude A, the frequency offset f_0, and the background. The difference $f_t - f_s$ is obtained from a double linear fit of 4 neighboring groups of values $f_0(t_0)$ after the ac Stark shift correction. A constant linear drift of the ECDL frequency is assumed during the recording of each 4 groups.

During 17 days of measurement in February–April 2008, about 1200 $1S$-$2S$ hydrogen spectra have been recorded in 28 sets (Fig. 2). Three types of tests were performed: (i) variation of the particle flow coming to the cold nozzle in the range $(0.8\text{–}10) \times 10^{17}\ \mathrm{s}^{-1}$, (ii) the quench field 2 switched on or off, and (iii) the direction of the compensation magnetic field is reversed. Further, we consider the most important systematic effects.

The collisional shift.—In 2003, we set the upper bound for the $2S$ HFS interval frequency shift as the total shift of the $2S$ level (8 MHz/mbar [12]). Now we theoretically reanalyze the shift which appears only in the third order of perturbation theory if collisions with H($1S$) are considered [18]. For each of the excited P states of the colliding partners a and b (m and n, correspondingly), the contribution to the shift of the $2S$ hyperfine component scales inversely to the sum $E^a_{2S} - E^a_{mP} + E^b_{1S} - E^b_{nP}$. The differential HFS shift is on the order of 10^{-7} of the $2S$ level shift due to the small ratio of the $2S$ HFS energy and the difference $E^b_{1S} - E^b_{nP}$. The short-range interaction does not contribute since, for impact parameters smaller than $20a_0$ (a_0 is the Bohr radius), the $2S$ state quenches. Integration over the discrete spectrum gives a result on the order of 10 Hz/mbar, and the continuum gives a similar contribution. The effect from collisions with H_2 should be of the same size because the closest dipole transition from the H_2 ground state lies is the UV region. The intrabeam pressure in the nozzle is 10^{-4} mbar and rapidly decreases in the expanding beam, so we can neglect the shift. A stronger effect may be induced by the dipole interaction with photoionized H [11]. Since there are only about 10 protons present in the excitation zone at a time, the effect is negligible.

We extrapolate the data of Fig. 2 to zero flow separately for each of the time bins. No systematic deviation between the extrapolated and the averaged values is observed. For $\tau = 810\ \mu$s, the difference equals 1 Hz with uncertainties of 11 and 6 Hz. The data taken at higher flows have an excessive scatter due to an instability of the overloaded cryogenic vacuum system, so we exclude them (shifting the final value by $+0.5\sigma$) from the analysis. The data are averaged without adding any systematics.

Line shape or beam temperature.—We analyze the averaged low- and moderate-flow data (Fig. 2) for different delays τ (Fig. 3, top) which shows an increase of the measured $f_{\mathrm{HFS}}(2S)$ frequency for shorter delays. The differential second-order Doppler effect is on the millihertz level and cannot explain the difference. The analysis of the line shapes indicates that the $2S(F = 0)$ atoms have a higher temperature T than the $2S(F = 1)$ ones (assuming a Maxwellian distribution). The amplitude ratio of the two hyperfine transitions varies from 3.1 to 3.6 depending on τ (see the inset) which means that the fraction of slow singlet atoms is less than for the triplet ones.

Fitting the singlet and triplet lines by line shapes simulated for different beam temperatures [17], we find for the difference $\Delta T = \langle T_s \rangle - \langle T_t \rangle = 0.4$ K with $\langle T_s \rangle = 4.2$ K. The thermalization of hydrogen atoms on the H_2 film depends on its spin state, which we still cannot explain.

We have evaluated the expected shift of $f_{\mathrm{HFS}}(2S)$ vs ΔT for different τ by Monte Carlo simulations. The dependencies are nearly linear with slopes of 220(40) Hz/K (10 μs), 68(5) Hz/K (210 μs), 17(4) Hz/K (410 μs), 5(3) Hz/K (610 μs), and 0(2) Hz/K for higher delays (Fig. 3). The uncertainties result from numerical errors and possible jitter of τ at a level of 20 μs. As expected,

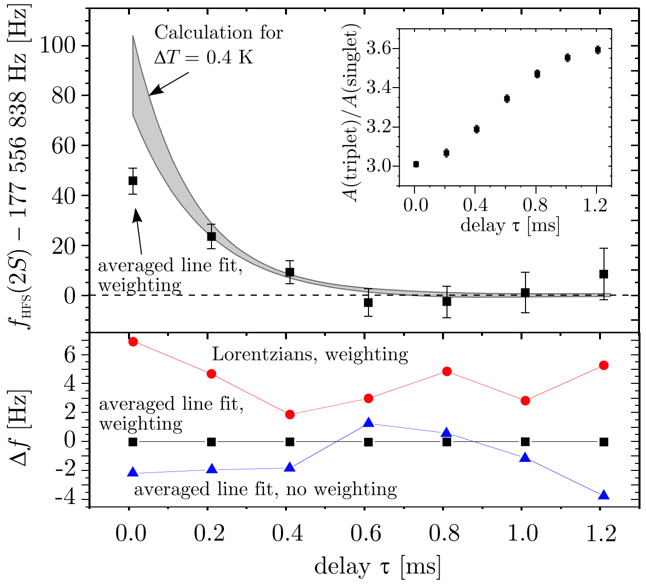

FIG. 3 (color online). Top: Averaged experimental $f_{\mathrm{HFS}}(2S)$ results for different τ (squares). Only low- and moderate-flow data from Fig. 2 are analyzed. The gray 1σ area shows the expected frequency shift for $\Delta T = 0.4$ K. Inset: The measured amplitude ratio of the triplet and singlet transitions which is consistent with $\Delta T = 0.4$ K. Bottom: Mutual deviation of averaged HFS interval frequencies for different evaluation methods. Error bars are similar to the ones from the upper plot.

TABLE I. Uncertainty budget for the new $2S$ HFS frequency measurement in atomic hydrogen.

	Frequency [Hz]	Uncertainty [Hz]
Averaged interval frequency	177 556 835.3	6.2
Line shape/temperature	0	2
dc Stark shift	−1	1
ac Stark shift	0	1.3
Magnetic fields	0	0.5
Final result	177 556 834.3	6.7

the effect vanishes at higher τ since the velocity distribution of the delayed atoms is insensitive to the initial distribution. The optimal compromise between the statistical uncertainty and the effect of different beam temperatures is reached at $\tau = 810\ \mu$s.

The influence of the fitting model and data weighting is analyzed in Fig. 3 (bottom). The Lorentzian fit of strongly asymmetrical spectra for $\tau = 10\ \mu$s results in a shift of 7(10) Hz. On the other hand, the line shape for $\tau = 810\ \mu$s is indistinguishable from a Lorentzian, so the effect reduces to the subhertz level. For $\tau = 810\ \mu$s, we get $f_{\text{HFS}}(2S)$ of 177 556 835.3(6.2) Hz and add 2 Hz uncertainty for line shape or beam temperature shifts.

The ac Stark shift.—The differential ac Stark shift of the $2S$ hyperfine components is negligible ($\sim 1\ \mu$Hz/mW [12]). Though the measured difference in singlet and triplet excitation powers is taken into account for each individual spectrum, the uncertainty of the correction itself may cause an error in $f_{\text{HFS}}(2S)$. Comparison of the data evaluated with or without correction shows a systematic difference from 2 to 5 Hz depending on the delay τ. By assuming an error in the ac Stark shift evaluation of 30% (including the error in the power measurement), the contribution to the final uncertainty budget is 1.3 Hz.

The dc Stark shift.—We have no possibility to measure stray electric fields in our apparatus and evaluate its contribution of $-1(1)$ Hz as in Ref. [12]. The influence of quench fields 1 and 2 is tested with the help of simulations [17], and an effect on the subhertz level is expected.

Magnetic fields.—The sensitivity of $f_{\text{HFS}}(2S)$ to an external magnetic field B equals $+9600B^2$ Hz/G^2. In 5 sets of measurements, the compensation field direction was inverted which increased the field in the less shielded zone from 30 to 300 mG (Fig. 2). The corresponding $f_{\text{HFS}}(2S)$ differs from the value measured with proper orientation by $-3(12)$ Hz at $\tau = 810\ \mu$s. We estimate the uncertainty resulting from magnetic fields as 0.5 Hz.

Summarizing the uncertainties (Table I), we get the final result $f_{\text{HFS}}(2S) = 177\,556\,834.3(6.7)$ Hz. The corresponding value $D_{21} = 48\,923(54)$ Hz is in good agreement with the theoretical prediction (Fig. 4), which is the first result after Ref. [8] consistent with theory within 1σ. This measurement is part of the long-term project on precision spectroscopy of the $1S$-$2S$ transition in H [16] and has an impact on its centroid frequency used for the Rydberg constant derivation [2].

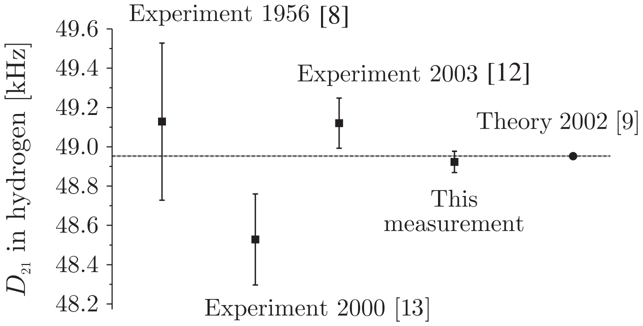

FIG. 4. Experimental and theoretical values for the $D_{21} = 8f_{\text{HFS}}(2S) - f_{\text{HFS}}(1S)$ difference in atomic hydrogen.

The work is supported in part by RSSF, MD-887.2008.2, DFG GZ 436 RUS 113/769/0-3, and RFFI 08-02-91969. J. A. is supported by the EU Marie Curie Fellowship. The authors are grateful to Th. Udem and G. Gabrielse for stimulating discussions.

---

[*] Also at P. N. Lebedev Physical Institute, Moscow, Russia.

[†] Also at D. I. Mendeleev Institute for Metrology, St. Petersburg, Russia.

[1] P. J. Mohr, B. N. Taylor, and D. B. Newell, Rev. Mod. Phys. **80**, 633 (2008).
[2] F. Biraben, arXiv:0809.2985v1.
[3] M. Hori *et al.*, Phys. Rev. Lett. **96**, 243401 (2006).
[4] M. I. Eides, H. Grotch, and V. A. Shelyuto, Phys. Rep. **342**, 63 (2001).
[5] S. G. Karshenboim, Phys. Rep. **422**, 1 (2005).
[6] D. E. Zwanziger, Phys. Rev. **121**, 1128 (1961).
[7] M. M. Sternheim, Phys. Rev. **130**, 211 (1963).
[8] J. W. Heberle, H. A. Reich, and P. Kusch, Phys. Rev. **101**, 612 (1956).
[9] S. G. Karshenboim and V. G. Ivanov, Phys. Lett. B **524**, 259 (2002); Eur. Phys. J. D **19**, 13 (2002).
[10] H. A. Schüssler *et al.*, Phys. Rev. **187**, 5 (1969).
[11] M. H. Prior and E. C. Wang, Phys. Rev. A **16**, 6 (1977).
[12] N. Kolachevsky, M. Fischer, S. G. Karshenboim, and T. W. Hänsch, Phys. Rev. Lett. **92**, 033003 (2004).
[13] N. E. Rothery and E. A. Hessels, Phys. Rev. A **61**, 044501 (2000).
[14] N. Ramsey, Hyperfine Interact. **81**, 97 (1993).
[15] J. Alnis, A. Matveev, N. Kolachevsky, T. Udem, and T. W. Hänsch, Phys. Rev. A **77**, 053809 (2008).
[16] M. Fischer *et al.*, Phys. Rev. Lett. **92**, 230802 (2004).
[17] N. Kolachevsky *et al.*, Phys. Rev. A **74**, 052504 (2006).
[18] C. M. Dutta, N. C. Dutta, and T. P. Das, Phys. Rev. A **2**, 30 (1970).